

# Application of ultrasonography and $^{99m}\text{Tc}$ -MIBI scintigraphy in the diagnosis and localization of hyperparathyroidism

Y. Luo<sup>1,2</sup>, C. Peng<sup>3</sup>, Q. Deng<sup>1</sup>, H. Song<sup>1</sup>, S. Zhai<sup>2\*</sup>, Q. Zhou<sup>1\*</sup>

<sup>1</sup>Department of Ultrasound Imaging, Renmin Hospital of Wuhan University, Wuhan, Hubei, 430060, China

<sup>2</sup>Department of Nuclear Medicine, Putuo People's Hospital, Tongji University, Shanghai, 200060, China

<sup>3</sup>Department of Medical Ultrasound, Shanghai Tenth People's Hospital, Shanghai, 200072, China

## ► Original article

### \*Corresponding author:

Qing Zhou & Shijun Zhai, Ph.D.,  
E-mail: zhouqing1619@163.com, zhaishijunprm@163.com

Received: May 2023

Final revised: July 2023

Accepted: August 2023

*Int. J. Radiat. Res.*, January 2024;  
22(1): 97-101

DOI: 10.52547/ijrr.21.1.14

**Keywords:** Ultrasonography,  $^{99m}\text{Tc}$ -MIBI, hyperparathyroidism, SPECT, CT

## INTRODUCTION

Hyperparathyroidism (HPT) is a group of clinical syndromes resulting from abnormal calcium and phosphorus metabolism caused by excessive parathyroid hormone (PTH) secretion by the parathyroid glands (PTGs) <sup>(1)</sup>. HPT can cause hypercalcemia, urinary and skeletal system disorders, and even organ failure in severe cases, endangering the life safety of patients <sup>(2)</sup>. At present, the pathogenesis of HPT has not been fully defined, and many factors such as genetic factors, alcohol consumption, head radiotherapy history, and living habits are all triggers <sup>(3)</sup>. As indicated by the World Health Organization (WHO) statistics, the incidence of HPT is increasing year by year in recent years, with the global new cases exceeding 2 million in the year 2020 alone <sup>(4)</sup>. Clinically, parathyroidectomy is recommended as the standard treatment for HPT, which can completely remove HPT nodules and provide definitive and long-lasting treatment; surgery-related complications are increasing in older patients <sup>(5)</sup>. As medical technology develops, minimally invasive treatment has gradually become a

## ABSTRACT

**Background:** To discuss the application value of ultrasonography (US) and  $^{99m}\text{Tc}$ -methoxyisobutylisonitrile ( $^{99m}\text{Tc}$ -MIBI) scintigraphy in hyperparathyroidism (HPT), so as to provide a more reliable guarantee for surgery or thermal ablation. **Materials and Methods:** Sixty-four HPT patients admitted to our hospital and the Tenth People's Hospital of Tongji University from January 2018 to February 2023 were selected as research participants. All patients underwent cervical US, dual-phase  $^{99m}\text{Tc}$ -MIBI planar scintigraphy, single photon emission computed tomography (SPECT), and pathological examination. The diagnostic efficiency of the above three imaging modalities was evaluated with pathological findings as the gold standard. In addition, the influence of parathyroid position, size and histological type on imaging results was evaluated.

**Results:** Among the 64 patients, 71 positive lesions were pathologically confirmed. The analysis showed that  $^{99m}\text{Tc}$ -MIBI SPECT/CT (Kappa=0.806) and US (Kappa=0.686) had high consistency with pathological findings, while dual-phase  $^{99m}\text{Tc}$ -MIBI planar scintigraphy had moderate consistency with pathological examination results (Kappa=0.594). **Conclusions:**  $^{99m}\text{Tc}$ -MIBI scintigraphy can significantly improve the diagnostic rate of parathyroid lesions. US is first recommended for patients suspected of HPT, followed by  $^{99m}\text{Tc}$ -MIBI scintigraphy for confirmation.

new choice for HPT treatment in recent years <sup>(6)</sup>. Of them, ultrasound-guided thermal ablation is a novel therapy for nodules in the breast, thyroid and other organs. For HPT, thermal ablation has also been demonstrated to be safer and more effective than open surgery <sup>(7)</sup>. However, for both thermal ablation and surgical treatment, the precise localization of parathyroid lesions before surgery is a key factor affecting the therapeutic effect <sup>(8)</sup>. Ultrasonography (US), dual-phase  $^{99m}\text{Tc}$ -methoxyisobutylisonitrile ( $^{99m}\text{Tc}$ -MIBI) planar scintigraphy, and single-photon emission computed tomography (SPECT)/computed tomography (CT) are the most commonly used HPT imaging modalities in clinical practice. Among them,  $^{99m}\text{Tc}$ -MIBI SPECT/CT can provide anatomical and functional information as well as fusion images of the two, providing more diagnostic information and is therefore increasing used in clinical practice <sup>(9, 10)</sup>.

This study retrospectively analyzed US and  $^{99m}\text{Tc}$ -MIBI scintigraphy findings in patients with HPT, aiming to further explore the application value of the two in HPT, and provide reference and guidance for better implementation of surgery or thermal ablation in the future.

## MATERIALS AND METHODS

### Patient information

This is a single-center, retrospective study of 64 HPT patients admitted to the Tenth People's Hospital of Tongji University from January 2018 to February 2023, which were selected as the study subjects. Patients (18 males and 46 females) ranged in age from 17 to 86 years, with an average age of (57.5±14.5) years. All subjects signed informed consent, and the study was conducted in strict accordance with the *Declaration of Helsinki*.

### Criteria for patient enrollment and exclusion

Inclusion criteria: Before treatment, all patients underwent neck US, dual-phase  $^{99m}\text{Tc}$ -MIBI planar scintigraphy, SPECT/CT, and pathological examination before treatment, all patients were treated with pre-treatment puncture biopsy or postoperative pathology to obtain pathologic results, with the examination interval less than 2 weeks and complete clinical data. Exclusion criteria: Those who had been diagnosed with HPT in other hospitals and undergone surgical treatment, as well as those with secondary HPT caused by chronic kidney disease were excluded. All patients had blood drawn for serum PTH and calcium determination before treatment, and the treatment was completed within one month after all the tests.

### Inspection methods

The patient's neck was explored in the supine position by GE-E9 color Doppler US (GE, USA) with a probe frequency of 5.0-12.0 MHz. The lesions were recorded and the ultrasonic images were analyzed by more than two senior attending physicians.  $^{99m}\text{Tc}$ -MIBI was supplied by Shanghai Atom Kexing Pharmaceutical Co., Ltd., with radiochemical purity over 95 percent. After intravenous administration of 370-555 megabecquerel (MBq)  $^{99m}\text{Tc}$ -MIBI, imaging was performed 20 minutes later, followed by a 2-hour delayed-phase imaging. And the chest elevation position, including the neck and upper chest, was scanned when ectopic PTGs were suspected. Immediately after the imaging was completed, SPECT/CT tomography and fusion imaging were performed with the Siemens double-probe SPECT/CT (Siemens, German) instrument equipped with a high-resolution and low-energy parallel-hole collimator for nuclide dual-phase acquisition: matrix: 128×128, energy peak: 140 KeV, count: 500 K, magnification: 3, and window width: 20%. During SPECT/CT fusion acquisition, the two probes were rotated 180°, with every 15s/6° as a frame, a matrix of 64\*64, a magnification of 1.5, a voltage of 140KV, a current of 120 mA, and a slice thickness of 2 mm.

### Result interpretation

All images were visually analyzed by two

experienced nuclear medicine physicians independently. In case of disagreement, the image was read by another senior physician, and a unified result was obtained through mutual discussion among the three physicians. Diagnostic criteria for positive results of dual-phase planar scintigraphy: abnormal radioactive concentration can be seen in both early phase and delayed phase lesions, or normal in early phase and radioactive concentration in delayed phase. Diagnostic criteria for positive results of  $^{99m}\text{Tc}$ -MIBI SPECT/CT imaging: focal radioactive concentration can be seen in the parathyroid region or ectopic region, with soft tissue density nodules in the corresponding sites on CT.

### Diagnostic efficiency calculation

Pathological findings were used as the gold standard to calculate the diagnostic efficiency. True positive (TP): tested positive with both the method used and the gold standard. False positive (FP): tested positive with the method used versus tested negative with the gold standard. True negative (TN): tested negative with both the method used and the gold standard. False negative (FN): tested negative with the method used versus tested positive with the gold standard. Sensitivity = true positive/(true positive + false negative) ×100%. Specificity = true negative/ (true negative + false positive) ×100%. Diagnostic coincidence rate = (true positive+true negative)/total number of people ×100%.

### Statistical analyses

Statistical analyses were realized via SPSS24.0. Quantitative and enumeration data were statistically described as (c±s) and [n (%)], respectively. The Chi-square test was used for comparisons of enumeration data. The diagnostic consistency was tested by the kappa test, with a kappa value of 0.41-0.60, 0.61-0.80, and 0.81-1.0 suggesting moderate, high, and complete consistency, respectively. A significance level of  $P<0.05$  was used in all analyses.

## RESULTS

### Pathological findings

Among the 64 patients, 71 positive lesions were pathologically confirmed. The lesion size was 0.5-2 cm, with an average of (1.42±0.75) cm. Table 1. Typical cases and manifestations are shown in figure 1.

**Table 1.** Results of pathological examination.

Projects	n	Percentage
Location of the parathyroid glands	Normal	64 90.14
	Anomalies	7 9.86
Size of parathyroid gland	Diameter <1cm	29 40.85
	Diameter ≥1cm	42 59.15
Histological types of parathyroid glands	Parathyroid adenoma	62 87.32
	Nodular hyperplasia	9 12.68

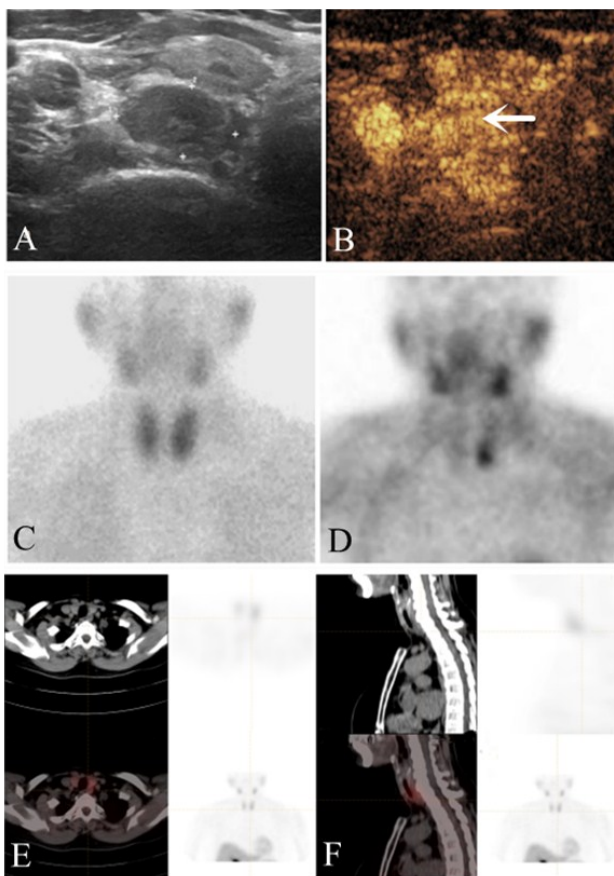


**Figure 1.** Imaging results. **A:** Two-dimensional ultrasonography showed a circular hypoechoic structure located infero-posterior to the inferior pole of the left thyroid lobe, with well-defined boundaries and a cross-sectional size of about 17 × 10 mm. **B:** Ultrasonography showed uniform and highly enhanced nodules (white arrow). **C, D:**  $^{99m}$ Tc-MIBI parathyroid scintigraphy revealed an abnormal concentration of the imaging agent in the inferior pole of the left thyroid lobe. **E, F:** The SPECT/CT tomosynthesis fusion system showed low-density soft tissue nodules located infero-posterior to the inferior pole of the left thyroid lobe, with well-defined boundaries and an abnormal concentration of the imaging agent.

**Table 2.** High concordance between  $^{99m}$ Tc-MIBI SPECT/CT and pathologic examination.

Pathological examination	Pathological		Total	Kappa	P	Sensitivity	Specificity	Diagnostic compliance rate	
	(+)	(-)							
$^{99m}$ Tc-MIBI SPECT/CT	(+)	63	3	0.806	<0.001	88.73	72.73	86.59	
	(-)	8	8						
<b>Total</b>		<b>71</b>	<b>11</b>						

99mTc-MIBI SPECT/CT:  $^{99m}$ Tc-methoxyisobutylisonitrile single photon emission computed tomography/computed tomography.

**Table 3.** Medium consistency between Dual-phase  $^{99m}$ Tc-MIBI planar scintigraphy and pathologic examination.

Pathological examination	Pathological		Total	Kappa	P	Sensitivity	Specificity	Diagnostic compliance rate	
	(+)	(-)							
Dual-phase $^{99m}$ Tc-MIBI planar scintigraphy	(+)	50	5	0.594	<0.001	70.42	54.55	68.29	
	(-)	21	6						
<b>Total</b>		<b>71</b>	<b>11</b>						

99mTc-MIBI:  $^{99m}$ Tc-methoxyisobutylisonitrile.

**Table 4.** High concordance between US and pathologic examination.

Pathological examination	Pathological		Total	Kappa	P	Sensitivity	Specificity	Diagnostic compliance rate	
	(+)	(-)							
US	(+)	56	4	0.686	<0.001	78.87	63.64	76.83	
	(-)	15	7						
<b>Total</b>		<b>71</b>	<b>11</b>						

US: ultrasonography.

### $^{99m}$ Tc-MIBI SPECT/CT imaging results

$^{99m}$ Tc-MIBI SPECT/CT detected 66 parathyroid lesions, of which 63 were TP, 3 were FP, 8 were TN, and 8 were FN. The diagnostic compliance rate of  $^{99m}$ Tc-MIBI SPECT/CT was 86.59%, which was highly consistent with the pathological findings as indicated by the Kappa test (Kappa=0.806, table 2).

### $^{99m}$ Tc-MIBI planar scintigraphy imaging results

Fifty-five lesions were detected by Dual-phase  $^{99m}$ Tc-MIBI planar scintigraphy, of which 50 were TP, 5 were FP, 6 were TN, and 21 were FN. The diagnostic coincidence rate was 68.29%, which was moderately consistent with the pathological findings (Kappa=0.594, table 3).

### US imaging results

US detected 60 parathyroid lesions, of which 56 were TP, 4 were FP, 7 were TN and 15 were FN. The diagnostic coincidence rate of 76.83% that was in high consistency with the pathological findings (Kappa=0.686, table 4).

## DISCUSSION

According to statistics, the current incidence of HPT is about 0.1%-0.4%, with a prevalence over 5% among women aged over 50<sup>(11)</sup>. Although the current clinical procedures such as surgery and thermal ablation can effectively cure HPT, accurate preoperative localization is still the key to the prognosis of patients<sup>(12)</sup>. In this study, we found that  $^{99m}$ Tc-MIBI SPECT/CT has a good effect in identifying HPT lesions, which can provide a more reliable guarantee for HPT treatment.

Studies have shown that  $^{99m}\text{Tc}$ -MIBI, being able to accumulate in the mitochondria of eosinophils in hyperparathyroid lesions, can be removed quickly by normal thyroid and parathyroid tissues, but slowly by hyperparathyroid tissues, so  $^{99m}\text{Tc}$ -MIBI in delayed phase can clearly display hyperparathyroid tissues<sup>(13)</sup>. However, dual-phase scintigraphy is a planar imaging, which has low sensitivity to some deep and small lesions; in addition, due to the small eosinophil count in parathyroid lesions, hemorrhage cystic degeneration in parathyroid adenomas and the expression of P-glycoprotein in the lesions, the uptake of MIBI by the lesions is reduced and eluted quickly, resulting in false negative<sup>(14)</sup>. It can be thus seen that  $^{99m}\text{Tc}$ -MIBI SPECT/CT has a better differential effect on PTH lesions. We believe that this is because  $^{99m}\text{Tc}$ -MIBI SPECT/CT is an organic fusion of functional imaging and anatomical imaging, in which SPECT technology can greatly improve image contrast and thus improve the detection rate of MIBI concentration, while CT can clearly display the neighbouring relationship between the lesion and the adjacent thyroid gland and other tissues, thus providing accurate localization information of lesions. Hence, SPECT/CT allows for simultaneous acquisition of functional information and accurate anatomical location of the lesions, which theoretically has higher diagnostic sensitivity and accuracy than planar imaging, especially for the detection of small adenomas<sup>(15)</sup>. Moreover, SPECT/CT imaging can effectively make up for the lack of accurate localization of lesions by dual-phase planar scintigraphy, while allowing for qualitative and localized diagnosis at the same time with one examination, greatly improving the diagnostic efficiency. In this study,  $^{99m}\text{Tc}$ -MIBI SPECT/CT had the best performance in detecting HPT lesions, showing the highest consistency with pathological findings, which can also support our view. Finally, with the development of US technology, the resolution of high-frequency ultrasound probe (10 MHz) has surpassed that of CT and magnetic resonance imaging (MRI), which can effectively evaluate the status of the PTG and become the first choice for screening parathyroid diseases<sup>(16)</sup>. However, the interpretation of US results largely depends on the operator's experience and awareness of the disease, which explains the wide variation in the sensitivity of US for HPT diagnosis in different studies<sup>(17, 18)</sup>. In this study, the differential effect of US on HPT was found to be slightly lower than that of  $^{99m}\text{Tc}$ -MIBI SPECT/CT, which may be influenced by the limited detection efficiency of US on ectopic parathyroid tissue or the subjective judgment of radiologists. Nonetheless, compared to  $^{99m}\text{Tc}$ -MIBI SPECT/CT, the safety of US is still one of its important advantages. Therefore, we can first perform US on patients suspected of HPT, and make confirmation with  $^{99m}\text{Tc}$ -MIBI SPECT/CT after finding suspicious

lesions, which can greatly improve the diagnostic efficiency of HPT lesions while ensuring the safety of patients. In our previous study, we also found that  $^{99m}\text{Tc}$ -MIBI SPECT/CT has a superior effect than CT for the diagnosis of renal cell carcinoma, which can support our results<sup>(19)</sup>. Meanwhile, in Li Q's study, they also mentioned that  $^{99m}\text{Tc}$ -MIBI SPECT/CT plays a key effect in the diagnosis of parathyroid adenoma, but US is still an essential examination<sup>(20)</sup>, which is also consistent with our view.

However, due to the limited experimental conditions, there are still many limitations to be addressed in this study. For example, we only used a single tracer of  $^{99m}\text{Tc}$ -MIBI and did not perform enhanced CT scanning, which may affect the detection of PTGs. Besides, it is necessary to strengthen the training of radiologists on interpreting HPT image results, so as to reduce the risk of missed diagnosis and misdiagnosis caused by human subjective factors. Finally, we also need to include more cases to further improve the reliability of the research results.

## CONCLUSION

$^{99m}\text{Tc}$ -MIBI SPECT/CT has a good diagnostic effect on HPT lesions, which can provide accurate preoperative localization for surgery or thermal ablation. However, in view of the higher clinical safety of US, we suggest that the suspected HPT patients should be examined by US first, and then supplemented by  $^{99m}\text{Tc}$ -MIBI SPECT/CT for confirmation, so as to provide a more reliable safety guarantee for the treatment and prognosis of patients.

## ACKNOWLEDGEMENTS

*I would like to express my gratitude to all those helped me during the writing of this thesis. I acknowledge the help of my colleagues, Songyuan Yu and Yuna Zhang, They have offered me suggestions in academic studies.*

## Declaration

**Ethical approval:** Not applicable.

**Consent to publish:** All authors gave final approval of the version to be published.

**Competing interests:** The authors report no conflict of interest.

**Author contributions:** Yangzi Luo: Methodology, Investigation, Data curation, original draft. Chengzhong Peng: Methodology, Investigation, Data curation, original draft. Qing Deng: Writing, review & editing. Hongning Song: Review & editing. Shijun Zhai: Idea, Supervision, review & editing. Qing Zhou: Idea, Supervision, review & editing.

**Availability of data and materials:** The data that support the findings of this study are available from

the corresponding author upon reasonable request.

**Funding:** Not applicable.

## REFERENCES

1. Bilezikian JP, Bandeira L, Khan A, Cusano NE (2018) Hyperparathyroidism. *Lancet*, **391**(10116): 168-178.
2. Lau WL, Obi Y, Kalantar-Zadeh K (2018) Parathyroidectomy in the Management of Secondary Hyperparathyroidism. *Clin J Am Soc Nephrol*, **13**(6): 952-961.
3. Kowalski GJ, Buta G, Żądło D, et al. (2020) Primary hyperparathyroidism. *Endokrynol Pol*, **71**(3): 260-270.
4. Messa P and Alfieri CM (2019) Secondary and Tertiary Hyperparathyroidism. *Front Horm Res*, **51**: 91-108.
5. Muñoz-Torres M and García-Martín A (2018) Primary hyperparathyroidism. Hipertrofia tiroidea primaria. *Med Clin (Barc)*, **150**(6): 226-232.
6. Cusano NE, Cipriani C, Bilezikian JP (2018) Management of normocalcemic primary hyperparathyroidism. *Best Pract Res Clin Endocrinol Metab*, **32**(6): 837-845.
7. Mizobuchi M, Ogata H, Koiwa F (2019) Secondary Hyperparathyroidism: Pathogenesis and Latest Treatment. *Ther Apher Dial*, **23**(4): 309-318.
8. Blau JE and Simonds WF (2021) Familial hyperparathyroidism. *Front Endocrinol (Lausanne)*, **12**: 623667.
9. Chen Z, Cheng L, Zhang W, He W (2022) Ultrasound-guided thermal ablation for hyperparathyroidism: current status and prospects. *Int J Hyperthermia*, **39**(1): 466-474.
10. Komek H, Yilmaz EE, Cakabay B, et al. (2018) Contrast enhanced [ $99m$ Tc] MIBI SPECT/CT in primary hyperparathyroidism. *Ann Ital Chir*, **89**: 379-384.
11. Newey PJ (2021) Hereditary Primary Hyperparathyroidism. *Endocrinol Metab Clin North Am*, **50**(4): 663-681.
12. Masi L (2019) Primary hyperparathyroidism, *Front Horm Res*, **51**: 1-12.
13. Fuster D, Torregrosa JV, Domenech B, et al. (2009) Dual-phase  $99m$ Tc-MIBI scintigraphy to assess calcimimetic effect in patients on haemodialysis with secondary hyperparathyroidism. *Nucl Med Commun*, **30**(11): 890-894.
14. Caldarella C, Treglia G, Pontecorvi A, Giordano A (2021) Diagnostic performance of planar scintigraphy using  $99m$ Tc-MIBI in patients with secondary hyperparathyroidism: a meta-analysis. *Ann Nucl Med*, **26**(10): 794-803.
15. Li X, Li J, Li Y, et al. (2020) The role of preoperative ultrasound, contrast-enhanced ultrasound, and  $99m$ Tc-MIBI scanning with single-photon emission computed tomography/X-ray computed tomography localization in refractory secondary hyperparathyroidism. *Clin Hemorheol Microcirc*, **75**(1): 35-46.
16. Zarei A, Karthik S, Chowdhury FU, et al. (2022) Multimodality imaging in primary hyperparathyroidism. *Clin Radiol*, **77**(6): e401-e416.
17. Salhi H, Bouziane T, Maaroufi M, et al. (2022) Primary hyperparathyroidism: Correlation between cervical ultrasound and MIBI scan. *Ann Afr Med*, **21**(2): 161-164.
18. Liu F, Liu Y, Peng C, et al. (2022) Ultrasound-guided microwave and radiofrequency ablation for primary hyperparathyroidism: a prospective, multicenter study. *Eur Radiol*, **32**(11): 7743-7754.
19. Zhao Q, Dong A, Zuo C, Yang B (2023)  $99m$ Tc-MIBI SPECT/CT in a case of renal oncocytosis. *Clin Nucl Med*, **10.1097/ RLU.000000000004775**.
20. Li Q, Pan J, Luo Q, et al. (2015) The key role of  $99m$ Tc-MIBI SPECT/CT in the diagnosis of parathyroid adenoma: a case report. *Arch Endocrinol Metab*, **59**(3): 265-9.

